Nanoscale Res Lett (2010) 5:1555–1560
DOI 10.1007/s11671-010-9676-0

NANO EXPRESS

Multi-Directional Growth of Aligned Carbon Nanotubes Over Catalyst Film Prepared by Atomic Layer Deposition

Kai Zhou · Jia-Qi Huang · Qiang Zhang · Fei Wei

Received: 18 May 2010 / Accepted: 12 June 2010 / Published online: 23 June 2010

Abstract The structure of vertically aligned carbon nanotubes (CNTs) severely depends on the properties of pre-prepared catalyst films. Aiming for the preparation of precisely controlled catalyst film, atomic layer deposition (ALD) was employed to deposit uniform Fe_2O_3 film for the growth of CNT arrays on planar substrate surfaces as well as the curved ones. Iron acetylacetonate and ozone were introduced into the reactor alternately as precursors to realize the formation of catalyst films. By varying the deposition cycles, uniform and smooth Fe_2O_3 catalyst films with different thicknesses were obtained on Si/SiO_2 substrate, which supported the growth of highly oriented few-walled CNT arrays. Utilizing the advantage of ALD process in coating non-planar surfaces, uniform catalyst films can also be successfully deposited onto quartz fibers. Aligned few-walled CNTs can be grafted on the quartz fibers, and they self-organized into a leaf-shaped structure due to the curved surface morphology. The growth of aligned CNTs on non-planar surfaces holds promise in constructing hierarchical CNT architectures in future.

Keywords Aligned carbon nanotubes · Atomic layer deposition · Chemical vapor deposition · Catalysis · Nanotechnology

Electronic supplementary material The online version of this article (doi:10.1007/s11671-010-9676-0) contains supplementary material, which is available to authorized users.

K. Zhou · J.-Q. Huang · Q. Zhang · F. Wei (✉)
Beijing Key Laboratory of Green Chemical Reaction Engineering and Technology, Department of Chemical Engineering, Tsinghua University, 100084 Beijing, China
e-mail: wf-dce@tsinghua.edu.cn

Introduction

Vertically aligned carbon nanotube (CNT) arrays were composed of aligned CNTs and possessed outstanding performances in materials science, catalysis, optics, electrics, and energy conversion/storage. Numerous functional applications, such as nano-brushes, field emitters, catalyst and catalyst supports, electronic electrodes, shock absorbing, energy conversion and storage, have been proposed [1–5]. The performance of aligned CNTs depends highly on the intrinsic structure of CNTs as well as the organization of CNTs. For example, large specific surface area (small CNT diameter and wall number) and suitable pore size distribution (hierarchical array structures) were required for the application of aligned CNT arrays in supercapacitor [6]. Therefore, the modulations of the CNT structure and their organization were of common interest in the research of CNT arrays.

Precisely controlled catalyst layers were widely used to modulate the metal catalyst particle size and therefore the structure of CNTs in the arrays. Generally, thin catalyst film favored the synthesis of CNTs with few walls. Physical vapor deposition (PVD, such as electron beam evaporation and magnetic sputtering) was one of the most popular methods for the deposition of uniform catalyst films on substrates [1, 7–9]. The wall number distribution of CNTs has been successfully controlled by modulating the thicknesses of Fe catalyst films [9]. Some endeavors on modulating the CNT structure by delicately controlled growth parameters were also made [10]. However, it must be noticed that, up to now, precise deposition of metal catalyst film on a non-planar surface was still difficult. Therefore, it is hard to synthesize aligned few-walled CNTs on a non-planar surface [11], which brings difficulties in constructing multi-stage aligned CNTs on non-planar substrates.

On the other hand, CNT arrays can be facilely synthesized on non-planar surfaces through floating catalyst chemical vapor deposition (CVD) [12]. Catalyst particles were in situ formed on substrates during the growth process of aligned CNTs [12–14]. Various functional materials with complex structures, such as CNT flowers [12, 15], CNT brushes [2, 16–18], CNT polyhedrons [19], CNT tubes [20, 21], have been fabricated. However, the catalyst particles formed by the decomposition of catalyst precursor were easily agglomerated into large ones and this gave rise to CNT arrays composed of large-diameter multi-walled CNTs (with diameters mainly in the range of 10–200 nm) [12]. Consequently, the as-obtained aligned CNTs were with limited specific surface area (lower than 200 m^2/g). This is still an obstacle for the further applications of hierarchical CNTs. Under the state-of-the-art of CNT array synthesis, the construction of multi-stage CNT arrays composed of thin CNTs on non-planar surface was still an obstacle. Considering the hardness in controlling catalyst sizes during floating catalyst process, a method for the uniform coating of catalysts on non-planar substrate should be developed.

Recently, atomic layer deposition (ALD) has become an important way to fabricate thin film on various substrates. It is a thin film growth method based on sequential, self-limiting surface reactions that can deposit conformal thin films with excellent conformal step coverage and is ideal for the deposition on complex non-planar surface topography [22, 23]. It is a powerful tool to fabricate thin film on irregular or porous substrate. For instance, Liu et al. reported the deposition of platinum nanoparticles on CNTs by ALD for the application in proton-exchange membrane fuel cells [24]; ALD was also employed to grow coaxial thin films of Al_2O_3 [25], V_2O_5, TiO_2, HfO_2, [26, 27], and Al_2O_3/W bilayers [25] on CNTs. Recently, Amama et al. reported the preparation of alumina layer as Fe catalyst support through ALD process for CNT growth. It should be noticed that the metal film was still prepared by electron beam evaporation [28]. Direct fabrication of metal catalyst film served as active phase for CNT growth is still an open question.

In this contribution, we developed a method using ALD to prepare uniform metal catalyst films for aligned CNT growth. As illustrated in Fig. 1, various kinds of substrates, such as wafers and quartz fibers, were selected as substrates for the deposition of Fe_2O_3 film by ALD. Iron acetylacetonate and ozone were introduced into the reactor alternately as precursors for the preparation of Fe_2O_3 films through the following chemical reaction:

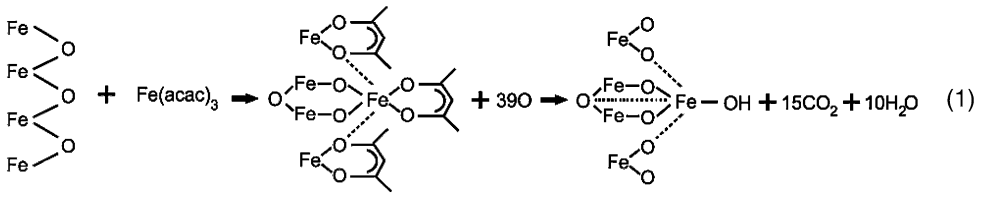

(1)

During ALD process, iron source was imported into the reactor and a self-terminating reaction occurred on the substrate surface. After a purging of inert gas N_2 to remove the non-reacted reactants and gaseous by-products, monolayer iron compounds were adsorbed. As ozone oxidized the iron compounds, monolayer iron oxides were obtained during a cycle. After a purge to evacuate ozone and by-products, the deposition process continued next cycle, and the thicknesses of Fe_2O_3 films were controlled by varying the reaction cycles. After the deposition of catalysts, the substrates were transferred into tubular furnace and annealed under hydrogen atmosphere to reduce iron oxides into Fe catalysts. The CVD process was then conducted for the growth of aligned few-walled CNTs. Since the catalyst films were deposited on all the surfaces exposed to the

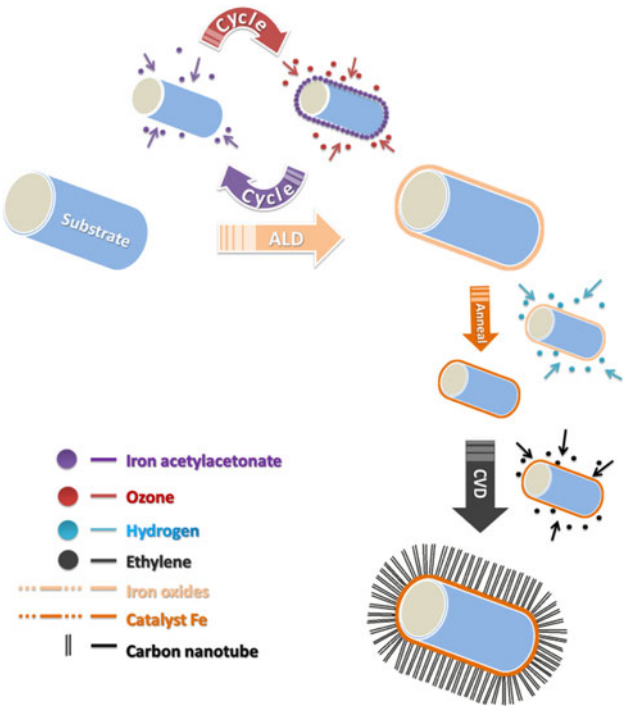

Fig. 1 Schematic illustration of the ALD and CVD process for the synthesis of CNT arrays

gaseous precursors in ALD process, few-walled CNT arrays can radially grow on fibrous substrates.

Experimental

Preparation of Catalyst Film by ALD Method

Silicon wafer (with 700 nm SiO_2 layer) coated with 10-nm-thick Al_2O_3 by e-beam evaporation and quartz fibers with a diameter of about 10 μm were employed as substrates for ALD deposition. The iron source was $Fe(acac)_3$ (iron(III) acetylacetonate, Alfar, >99.99%) and ozone served as oxidants was supplied from an ozone generator with oxygen (Beiwen Gas, purity >99.999%) as input. The output ozone concentration is 7 vol%. N_2 was used as both carrier gas for iron source and the purge gas for ALD deposition.

Thin catalyst films were deposited in a 3 L vacuum chamber. The precursors (iron sources and oxidants) were pulsed alternately into the reactor, separated by N_2 gas purge (purity > 99.999%) to realize the ALD deposition. The films were deposited at a pressure of about 100–500 Pa in the temperature of 230°C. The iron source was sublimed at 80°C and carried into the reactor by N_2. Each ALD cycle consisted of 100-s $Fe(acac)_3$ pulse, 3-s N_2 purge pulse, 10-s ozone pulse, and 3-s N_2 purge pulse. Various cycles of ALD deposition were conducted on both wafer and quartz fiber to obtain Fe_2O_3 catalyst films.

Synthesis of Aligned CNTs on ALD Catalysts

Substrates were transferred into horizontal quartz-tube-reactor set in a tube furnace for the CVD synthesis of aligned CNTs. The temperature of the reactor increased to 750°C under the protection of Ar and H_2. C_2H_4 together with CO_2 was then introduced to realize the growth of CNT arrays. The typical flow rates of Ar, H_2, C_2H_4, and CO_2 were 250, 200, 100, and 50 sccm, respectively. After a 1-h growth of aligned CNTs, the feedstock of C_2H_4 and CO_2 was terminated, and the reactor was cooled down under the protection of Ar and H_2.

Characterization

The catalyst layers deposited by ALD process were characterized with X-ray photoelectron spectroscopy (XPS, PHI Quantera SXM) and atomic force microscope (AFM, Nanoman VS). High-resolution scanning electron microscopy (SEM, JSM 7401F operating at 5.0 kV) was used to characterize the morphology of the CNT arrays. High-resolution transmission electron microscopy (TEM, JEM 2010 operating at 120.0 kV) was used to determine the detailed structure of the CNTs in the arrays. Raman spectroscopy of the CNTs was performed using a Raman microscope (Renishaw, RM2000, He–Ne laser excitation line 633.0 nm).

Results and Discussion

Silicon wafer was selected as a model substrate to demonstrate the deposition of Fe_2O_3 film and the synthesis of aligned CNTs. To confirm the deposition of Fe_2O_3 film by ALD, XPS was collected from the Fe_2O_3/Al_2O_3(10 nm)/SiO_2(700 nm)/Si substrate. O, Al, and Fe elements can be detected (Fig. 2a). The XPS data of different ALD cycles revealed a positive relationship between the Fe content and the ALD cycle number (Fig. 2b). An Fe abundance of *ca.* 1% was detected on the surface of Fe_2O_3/Al_2O_3(10 nm)/SiO_2(700 nm)/Si obtained by 10 ALD cycles. It increased to over 6% after 40 ALD cycles. This confirmed that the Fe has been successfully deposited and the thickness of Fe_2O_3 film on the surface increased with ALD cycles. As the growth of CNT arrays was sensitive to the surface morphologies of substrates, the planarity after ALD deposition was also investigated using AFM. Figure S1a showed the AFM topography images of original silicon substrate with Al_2O_3 barrier layer and the substrate with 10, 20, 30 ALD

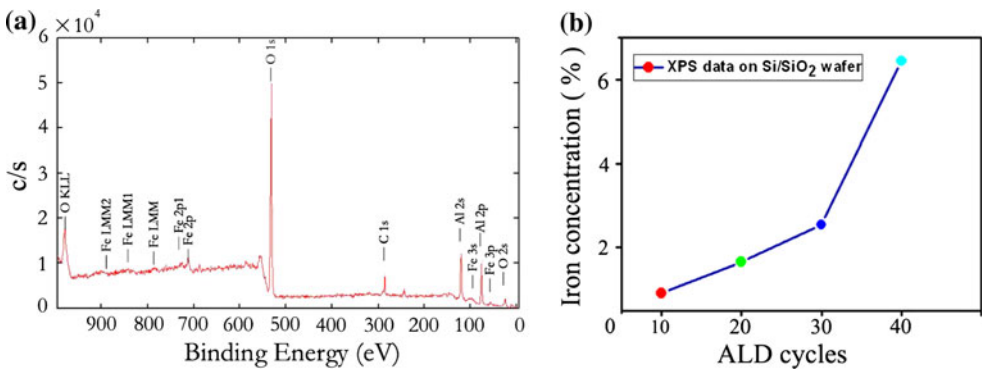

Fig. 2 **a** Typical XPS data on substrate surface with Fe_2O_3 deposited by 30 ALD cycles; **b** Iron concentration at the surface of Fe_2O_3/Al_2O_3(10 nm)/SiO_2(700 nm)/Si after different ALD cycles

cycles. The original substrate showed a relatively smooth and uniform surface, and only a few particles can be observed, showing high planarity of the thin Al_2O_3 film. A few small particles were generated on the substrate surface during the ALD process. The average roughness increased gradually from 0.15 to 0.30 nm with the ALD cycles increasing from 0 to 30 cycles. Though the roughness of substrate increased slightly, it maintained good planarity for the growth of aligned CNTs.

After the deposition of Fe_2O_3 films on silicon wafer, CVD growth was conducted. Figure 3a showed the as-obtained aligned CNTs on substrate with 40 ALD cycles for catalyst deposition, which possessed a uniform top surface. After the reduction of metal catalysts and the introduction of carbon source, high-density Fe nanoparticles formed, and aligned CNTs synchronously grew on the wafer. Figure 3b showed the CNT arrays on both the top surface (with Al_2O_3 barrier layer) and side cross-section (without SiO_2 and Al_2O_3 barrier layer). The height of CNT arrays on the top surface (200 μm) was much higher compared with that on the side cross-section (30 μm) due to the existence of barrier layers. As reported previously, the barrier layers can supply more nucleation sites on the surface by increasing the surface roughness and to resist the sintering of Fe nanoparticles due to the stronger substrate catalyst interaction [29–31]. Radial growth of CNTs on a wafer illustrated in Fig. 3b suggested that the Fe catalyst film was coated onto all the surfaces of the substrate. Thus, uniform catalyst films on all surfaces of substrate can be deposited by ALD, which provides a facile way to prepare catalyst film for multi-directional growth of aligned CNTs.

TEM characterization was performed to determine the detailed structure of CNTs in the arrays. Figure 3d is the typical low-magnification TEM image of the CNTs derived on the substrate with 40 ALD cycles of Fe_2O_3 deposition. The samples mainly consisted of few-walled CNTs. Figure 3e showed a triple-walled CNT with an outer diameter of 8.7 nm. Based on the statistic results, CNTs obtained with different ALD cycles for Fe_2O_3 deposition showed outer diameters ranging from 7 to 12 nm and wall numbers of 3-6. The top part of CNT arrays with different ALD cycles was further examined by Raman spectroscopy (Fig. 3f). The Raman spectra showed two main peaks: D peak around 1,325 cm^{-1} and G peak around 1,580 cm^{-1}, corresponding to the signal of disordered and ordered graphite structures. Therefore, the intensity ratio of G peak to D peak was widely used in determining the graphitization degree of CNTs. As calculated, the I_G/I_D ratio kept at about 0.72 for the CNTs derived on substrate with 10- to 30-ALD cycle catalyst film. The relatively low I_G/I_D ratio may be attributed to the large diameters and high defect densities of the CNTs [10]. The I_G/I_D ratio decreased to 0.58 for the CNT arrays obtained on substrates with 40 ALD cycles, which can be attributed to higher surface roughness and the non-uniform catalyst particles.

The synthesis of CNT arrays on non-planar surfaces was important to explore the applications of CNTs in composites, electrodes, biology and catalyst supports. Due to the difficulty in the preparations of uniform catalyst layers through PVD process on non-planar surfaces, the synthesis of uniform aligned CNTs on all surface of substrate was only achieved by floating catalyst process and impregnation process [2, 16, 32–34]. Yamamotoa et al. [32] soaked

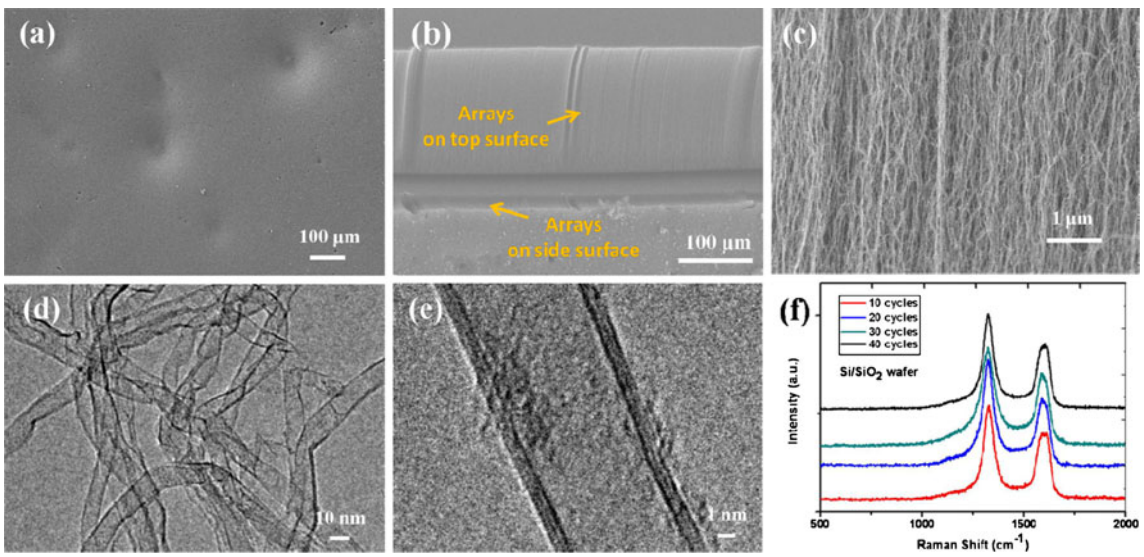

Fig. 3 **a** Top surface of uniform aligned CNTs grown on wafer; **b** Aligned CNTs grown on top and side surface of wafer; **c** High-magnification SEM image of aligned CNTs; **d** Low- and **e** high-magnification TEM images of CNTs grown on wafer with 40 ALD cycles; **f** Raman spectrum of aligned CNTs grown on Si wafer with different ALD cycles

ceramic fibers in a solution of iron nitrate and placed fibers into tube furnace for CVD process. Radial growth of aligned multi-walled CNTs with an outer diameter of 17.1 nm was realized [32]. However, catalyst preparation for the growth of few-walled CNTs arrays on curved surface was still a challenge. Inspired by the growth of CNTs on all the surfaces of Si wafers, we conducted the ALD deposition of Fe_2O_3 catalyst on the quartz fiber with a diameter of about 10 μm and realized the synthesis of uniform few-walled CNT arrays on the curved surface. As shown in Fig. 4a, though the surface was composed of SiO_2 without Al_2O_3 layer, long CNT arrays (over 100 μm) formed on these thin fibers and self-organized into leaf-shaped morphologies. The side view of the CNT leaf showed a vertically aligned film structure (Fig. 4b), in which the top of CNTs assembled together and the roots attached to the quartz fibers. As the catalyst films were uniformly deposited on the curved surfaces, CNTs formed all around the quartz fiber and connected with each other into a woven structure when CVD growth started, which supported the following growth of CNT arrays. However, when the aligned CNTs began to grow, the stress accumulated on the top woven structure of CNTs due to the extended surface area of the aligned CNTs. Consequently, the CNT woven structure on the top of arrays ruptured, and a continuous gap would form along the axis of the quartz fiber. The further growth of aligned CNTs would drag the CNTs into the main growth direction (opposite to the ruptured gap), which led to the formation of leaf-shaped CNT arrays. TEM characterizations confirmed that the CNTs in this structure were mainly double- and triple-walled CNTs with outer diameters of less than 10 nm. Compared with previously reported multi-walled CNT structures (CNT brushes, CNT flowers, etc.), the CNTs prepared in this method were much thinner, longer, and more flexible, which caused the formation of leaf-like structures. The Raman spectra showed an I_G/I_D ratio of 0.89 for 10–30 ALD cycles of catalyst layers, which decreased to 0.74 for the 40-cycle ALD substrate. The relationship between the I_G/I_D ratio and the ALD cycle number was similar to those obtained on the silicon wafers.

The ALD process for the deposition of catalyst films realized the synthesis of few-walled CNT arrays on multi-shaped substrate. As demonstrated by the quartz fibers,

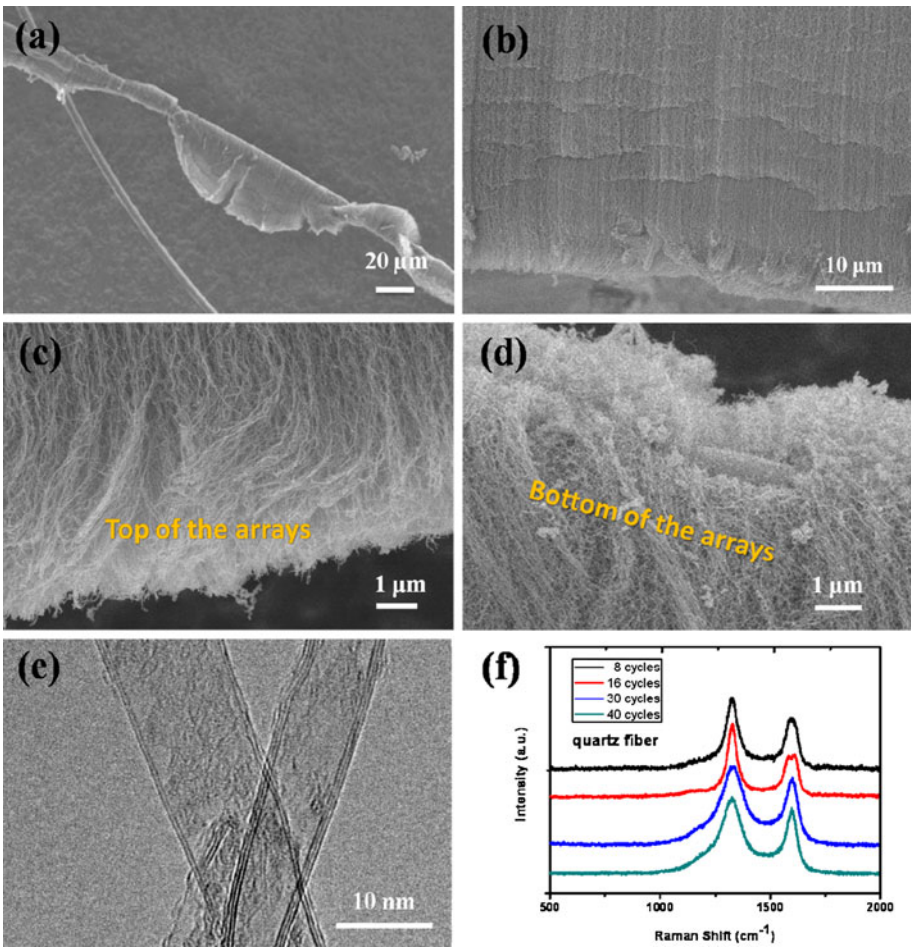

Fig. 4 **a** Low- and **b** high-magnification SEM images of aligned CNTs grown on quartz fiber; Morphologies of **c** top and **d** bottom of aligned CNTs grown on quartz fibers; **e** TEM images of few-walled CNTs from arrays on quartz fiber with 30 ALD cycles; **f** Raman spectra of CNTs arrays grown on quartz fibers with different ALD cycles

CNT arrays can radially grow on the fibers, which may find applications in the reinforcement in various cloths of fibers by CNTs [16, 32]. The growth of long CNT arrays may realize the multi-stage weaving of CNTs and the original fibers to construct 3D CNT architectures. Furthermore, it should be noticed that the leaf-like growth mode exposed the substrate (the catalyst particles) to the reaction atmosphere. The normally considered diffusion limitation and stress-induced deactivation for CNT arrays growth no longer existed, which provides an access to the formation of ultra-long aligned CNTs. The introduction of ALD in the synthesis of CNTs may bring applications in hierarchical electrode materials, micro-channel catalyst supports, pore-structure-designed membranes for multi-functional materials, catalysis, and energy conversion/storage [1, 4, 35].

Conclusions

ALD process was introduced for the preparation of uniform catalyst films for aligned CNT growth. With various ALD cycles, Fe_2O_3 films with different thicknesses were coated onto the substrate and supported the growth of few-walled CNT arrays. When on flat substrate, such as Si wafer, large area uniform aligned CNTs were fabricated, while aligned CNTs radially grew and self-organized into leaf-like structures on quartz fibers. Benefiting from the advantages in the precise control of film thickness and ability for coating substrate with complicated structures, ALD process holds potential applications for building up hierarchical CNT structures in future.

Acknowledgments The work was supported by the National Natural Science Foundation of China (Nos. 20736007, and 2007AA03Z346) and the China National Basic Research Program (No. 2006CB0N0702). We thank Prof. Dezheng Wang for his great help in the construction of ALD reaction chamber.

References

1. S.S. Fan, M.G. Chapline, N.R. Franklin, T.W. Tombler, A.M. Cassell, H.J. Dai, Science **283**, 512 (1999)
2. A.Y. Cao, V.P. Veedu, X.S. Li, Z.L. Yao, M.N. Ghasemi-Nejhad, P.M. Ajayan, Nat. Mater. **4**, 540 (2005)
3. J. Zhang, X. Liu, R. Blume, A.H. Zhang, R. Schlogl, D.S. Su, Science **322**, 73 (2008)
4. H. Pan, J.Y. Li, Y.P. Feng, Nanoscale Res. Lett. **5**, 654 (2010)
5. Q. Zhang, M.Q. Zhao, Y. Liu, A.Y. Cao, W.Z. Qian, Y.F. Lu, F. Wei, Adv. Mater. **21**, 2876 (2009)
6. T. Hiraoka, A. Izadi-Najafabadi, T. Yamada, D.N. Futaba, S. Yasuda, O. Tanaike, H. Hatori, M. Yumura, S. Iijima, K. Hata, Adv. Funct. Mater. **20**, 422 (2010)
7. K. Hata, D.N. Futaba, K. Mizuno, T. Namai, M. Yumura, S. Iijima, Science **306**, 1362 (2004)
8. C.L. Pint, N.T. Alvarez, R.H. Hauge, Nano Res. **2**, 526 (2009)
9. S. Chakrabarti, H. Kume, L.J. Pan, T. Nagasaka, Y. Nakayama, J. Phys. Chem. C **111**, 1929 (2007)
10. J.Q. Huang, Q. Zhang, M.Q. Zhao, F. Wei, Nano Res. **2**, 872 (2009)
11. H.S. Kim, B. Kim, B. Lee, H. Chung, C.J. Lee, H.G. Yoon, W. Kim, J. Phys. Chem. C **113**, 17983 (2009)
12. Q. Zhang, J.Q. Huang, M.Q. Zhao, W.Z. Qian, Y. Wang, F. Wei, Carbon **46**, 1152 (2008)
13. T.X. Cui, R.T. Lv, F.Y. Kang, Q. Hu, J.L. Gu, K.L. Wang, D.H. Wu, Nanoscale Res. Lett. **5**, 941 (2010)
14. R.T. Lv, F.Y. Kang, D. Zhu, Y.Q. Zhu, X.C. Gui, J.Q. Wei, J.L. Gu, D.J. Li, K.L. Wang, D.H. Wu, Carbon **47**, 2709 (2009)
15. D.L. He, M. Bozlar, M. Genestoux, J.B. Bai, Carbon **48**, 1159 (2010)
16. Q. Zhang, W.Z. Qian, R. Xiang, Z. Yang, G.H. Luo, Y. Wang, F. Wei, Mater. Chem. Phys. **107**, 317 (2008)
17. K. Konig, S. Novak, A. Ivekovic, K. Rade, D.C. Meng, A.R. Boccaccini, S. Kobe, J. Eur. Ceram. Soc. **30**, 1131 (2010)
18. H. Qian, A. Bismarck, E.S. Greenhalgh, M.S.P. Shaffer, Carbon **48**, 277 (2010)
19. J.Y. Qu, Z.B. Zhao, J.S. Qiu, Y. Gogotsi, Chem. Commun. **2747** (2008)
20. J.Y. Qu, Z.B. Zhao, Z.Y. Wang, X.Z. Wang, J.S. Qiu, Carbon **48**, 1465 (2010)
21. Z.B. Zhao, J.Y. Qu, J.S. Qiu, X.Z. Wang, Z.Y. Wang, Chem. Commun. **594** (2006)
22. M. Knez, K. Niesch, L. Niinisto, Adv. Mater. **19**, 3425 (2007)
23. S.M. George, Chem. Rev. **110**, 111 (2010)
24. C. Liu, C.C. Wang, C.C. Kei, Y.C. Hsueh, T.P. Perng, Small **5**, 1535 (2009)
25. A.S. Cavanagh, C.A. Wilson, A.W. Weimer, S.M. George, Nanotechnology **20**, 255602 (2009)
26. M.G. Willinger, G. Neri, E. Rauwel, A. Bonavita, G. Micali, N. Pinna, Nano Lett. **8**, 4201 (2008)
27. M.G. Willinger, G. Neri, A. Bonavita, G. Micali, E. Rauwel, T. Herntrich, N. Pinna, Phys. Chem. Chem. Phys. **11**, 3615 (2009)
28. P.B. Amama, C.L. Pint, S.M. Kim, L. McJilton, K.G. Eyink, E.A. Stach, R.H. Hauge, B. Maruyama, ACS Nano **4**, 895 (2010)
29. T. de los Arcos, M.G. Garnier, P. Oelhafen, D. Mathys, J.W. Seo, C. Domingo, J.V. Garci-Ramos, S. Sanchez-Cortes, *Carbon* **42,** 187 (2004)
30. J.B.A. Kpetsu, P. Jedrzejowski, C. Cote, A. Sarkissian, P. Merel, P. Laou, S. Paradis, S. Desilets, H. Liu, X.L. Sun, Nanoscale Res. Lett. **5**, 539 (2010)
31. J. Garcia-Cespedes, S. Thomasson, K.B.K. Teo, I.A. Kinloch, W.I. Milne, E. Pascual, E. Bertran, Carbon **47**, 613 (2009)
32. N. Yamamoto, A.J. Hart, E.J. Garcia, S.S. Wicks, H.M. Duong, A.H. Slocum, B.L. Wardle, Carbon **47**, 551 (2009)
33. E.J. Garcia, B.L. Wardle, A.J. Hart, N. Yamamoto, Compos. Sci. Technol. **68**, 2034 (2008)
34. Q.H. Zhang, J.W. Liu, R. Sager, L.M. Dai, J. Baur, Compos. Sci. Technol. **69**, 594 (2009)
35. D.S. Su, R. Schlogl, ChemSusChem **3**, 136 (2010)